Naval Research Laboratory

Washington, DC 20375-5320

Airborne Surface Backscattering Strength Measurements in the Western Atlantic Ocean

JOHN P. CROCKETT
PETER M. OGDEN
FRED T. ERSKINE

Acoustic Systems Branch
Acoustics Division

September 17, 1993

REPORT DOCUMENTATION PAGE

Public reporting burden for this collection of information is estimated to average 1 hour per response, including the time for reviewing instructions, searching existing data sources, gathering and maintaining the data needed, and completing and reviewing the collection of information. Send comments regarding this burden estimate or any other aspect of this collection of information, including suggestions for reducing this burden, to Washington Headquarters Services, Directorate for Information Operations and Reports, 1215 Jefferson Davis Highway, Suite 1204, Arlington, VA 22202-4302, and to the Office of Management and Budget. Paperwork Reduction Project (0704-0188), Washington, DC 20503.

1. AGENCY USE ONLY (Leave Blank)	2. REPORT DATE September 17, 1993	3. REPORT TYPE AND DATES COVERED Final

4. TITLE AND SUBTITLE Airborne Surface Backscattering Strength Measurements in the Western Atlantic Ocean	5. FUNDING NUMBERS PE - 62435N PR - R035B03
6. AUTHOR(S) John P. Crockett, Peter M. Ogden, and Fred T. Erskine	

7. PERFORMING ORGANIZATION NAME(S) AND ADDRESS(ES) Naval Research Laboratory Washington, DC 20375-5320	8. PERFORMING ORGANIZATION REPORT NUMBER NRL/FR/7142--93-9563

9. SPONSORING/MONITORING AGENCY NAME(S) AND ADDRESS(ES) Office of Naval Technology Arlington, VA 22217-5000	10. SPONSORING/MONITORING AGENCY REPORT NUMBER

11. SUPPLEMENTARY NOTES

12a. DISTRIBUTION/AVAILABILITY STATEMENT Approved for public release; distribution unlimited.	12b. DISTRIBUTION CODE

13. ABSTRACT (Maximum 200 words)

This report presents the results from a series of airborne, SUS-based acoustic surface backscattering strength tests conducted over the western Atlantic Ocean during April 1988. We describe the airborne technique used to gather the acoustic data and the environmental data (sound speed profiles and wind speed). Analysis provides information on sea surface acoustic backscattering strengths for mean grazing angles from 7° to 30°, wind speeds from 7 to 18 m/s, and frequencies from 50 to 800 Hz. The data analysis procedure is outlined, and the results are compared to first-order perturbation theory (air-water interface scatter), the Chapman-Harris empirical formula, and the Ogden-Erskine empirical algorithm. The absolute error in measured scattering strengths is approximately ±5 dB. The data comparison emphasizes the use of wind history as an environmental predictor of surface scattering. The results are summarized, and a list of the lessons learned concerning the experimental technique is provided. Brief analyses of the sound speed profiles and wind speed data are appended.

14. SUBJECT TERMS			15. NUMBER OF PAGES 36
Surface scattering Airborne technique Perturbation theory	Chapman-Harris Ogden-Erskine Environmental descriptor	Wind speed/wind history	16. PRICE CODE

17. SECURITY CLASSIFICATION OF REPORT UNCLASSIFIED	18. SECURITY CLASSIFICATION OF THIS PAGE UNCLASSIFIED	19. SECURITY CLASSIFICATION OF ABSTRACT UNCLASSIFIED	20. LIMITATION OF ABSTRACT UL

NSN 7540-01-280-5500

CONTENTS

AIRBORNE SURFACE BACKSCATTERING STRENGTH MEASUREMENTS IN THE WESTERN ATLANTIC OCEAN

INTRODUCTION

In April 1988, the Naval Research Laboratory (NRL) conducted a series of airborne acoustic surface backscattering strength tests over the western Atlantic Ocean. These tests had two purposes. First, they provided the means to further refine a technique of airborne, personal computer based, recording and measuring of low-frequency acoustic backscatter using signal underwater sound (SUS) charges. This technique meets the Navy need to perform acoustic surveys of surface and bottom scattering strengths below 1000 Hz with the ability to sample many sites in a relatively short span of time as compared to ship-based surveys. Second, the tests yielded measurements of surface scattering strength vs grazing angle and frequency, for a variety of wind speeds, as part of a continuing program at NRL to understand the nature of surface reverberation and to refine surface scattering prediction algorithms.

In this report, we give a description of the methodology used to acquire and analyze the April 1988 data, and we present a summary of the data collected. We then present the surface scattering strength results, along with the lessons learned about the use of the airborne technique to measure reverberation. In Appendix A, we present the in-situ sound speed profiles acquired during the tests. In Appendix B, we discuss the wind speed measurements used in the analysis.

EXPERIMENTAL METHOD

Airborne Technique

The aircraft from which the tests were conducted was a U.S. Navy P-3A, based at NRL's Flight Support Detachment Facility, Naval Air Station, Patuxent, Maryland. The acoustic sources used during the tests were Mk61 SUS charges set to detonate at a depth of 244 m. The receivers were AN/SSQ-57A sonobuoys, some of which had been modified at NRL to incorporate post-hydrophone attenuations of 20, 40, and 60 dB. This was done because AN/SSQ-57A sonobuoys have a limited dynamic range. By modifying them for different sensitivities and using results from sonobuoys with a range of attenuations, we attained an increase in the effective dynamic range with which to measure reverberation. The hydrophones of all sonobuoys deployed to a depth of 121 m.

Seven flights were conducted on separate days, and tests were carried out at either one or two sites on each flight. Upon arrival at a site, the aircraft descended to an altitude of approximately 90 m and deployed a Mk58 smoke marker, four sonobuoys (0, 20, 40, and 60 dB attenuations), and another Mk58 smoke marker. Because only one object could be launched at a time, this method resulted in at least 100-m separations between each sonobuoy. Sometimes up to six sonobuoys were deployed at one time. Usually incorporating 20 and 40 dB attenuations, the two extra sonobuoys were backup receivers to the four primary sonobuoys. Once the sonobuoys were deployed, the aircraft passed over the site to verify

---

that each receiver was functioning properly. The P-3A then flew a modified figure-eight flight pattern, centered on the sonobuoys. A single SUS charge, or "shot," was launched from the aircraft when the P-3A was judged to be near the center of the figure-eight. This judgment was based on two factors: the aircraft's On Top Position Indicator (OTPI) system and the visually estimated positions of the smoke markers. Once a shot was deployed, the aircraft flew straight and level until the reverberation had been received and recorded for a fixed amount of time. The aircraft then looped back in order to deploy another shot. This procedure continued until a site's complement of sources was used, typically 10 to 30 SUS charges. Figure 1 shows the geometry of the tests as outlined above.
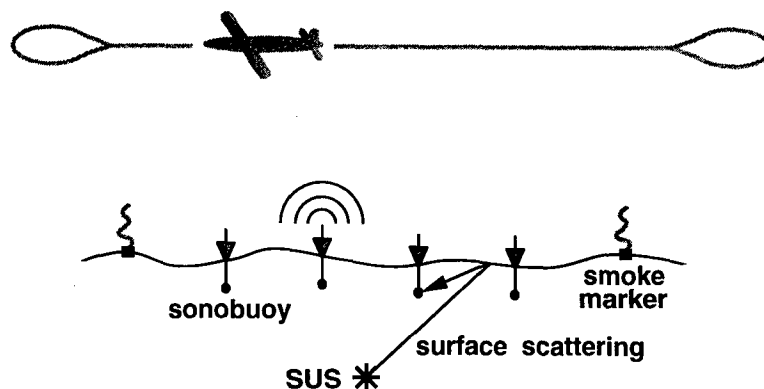

Fig. 1 — Experimental geometry of the airborne technique

The reverberation from each shot was recorded on four radio-frequency (RF) channels, each channel corresponding to a single sonobuoy's transmitter. The signals from the sonobuoys were digitized in real time on a PC/AT using four 2-kHz A/D converters; the outputs were stored on Bernoulli disks. The analog signals were also recorded on magnetic tape as backup. For those times when six sonobuoys were launched, only the analog backups contained all six sonobuoys' received reverberation; two channels could not be digitized in real time. After each shot had been recorded, each channel's digitized data were plotted in near real time to verify the data quality. Figure 2 shows an example of such a data display, taken from Flight 7, Site C.

Environmental Measurements

Wind speed and sound speed profiles were measured at each site; sea state was estimated visually from the cockpit. Wind speed information was gathered from two sources: a wind speed measuring system aboard the P-3A and NOAA meteorological buoys. NOAA maintains meteorological buoys along the eastern coast of the United States. The buoys record data such as air temperature, ocean temperature, wind speed, and relative humidity. Two of these buoys, Nos. 44004 and 41002, were moored in the general area of two of the test sites. After a site's SUS deployment phase, airborne expendable bathythermograph buoys (AXBTs) were dropped from the P-3A to measure the local sound speed profile. The in-situ sound speed profiles were extended to greater depths in post-test processing by merging them with archival sound speed profiles from the NAVOCEANO Generalized Digital Environmental Model (GDEM) database (1987).

Figure 3 shows the locations of both NOAA meteorological buoys and the sites where tests were performed. Table 1 shows a summary of the flights and test sites visited, noting the ocean depth, sea state, and average wind speed. Figure 4 shows a composite of sound speed profiles for all the flights and test sites. It can be seen from this figure that two distinct types of sound speed profiles existed at the test
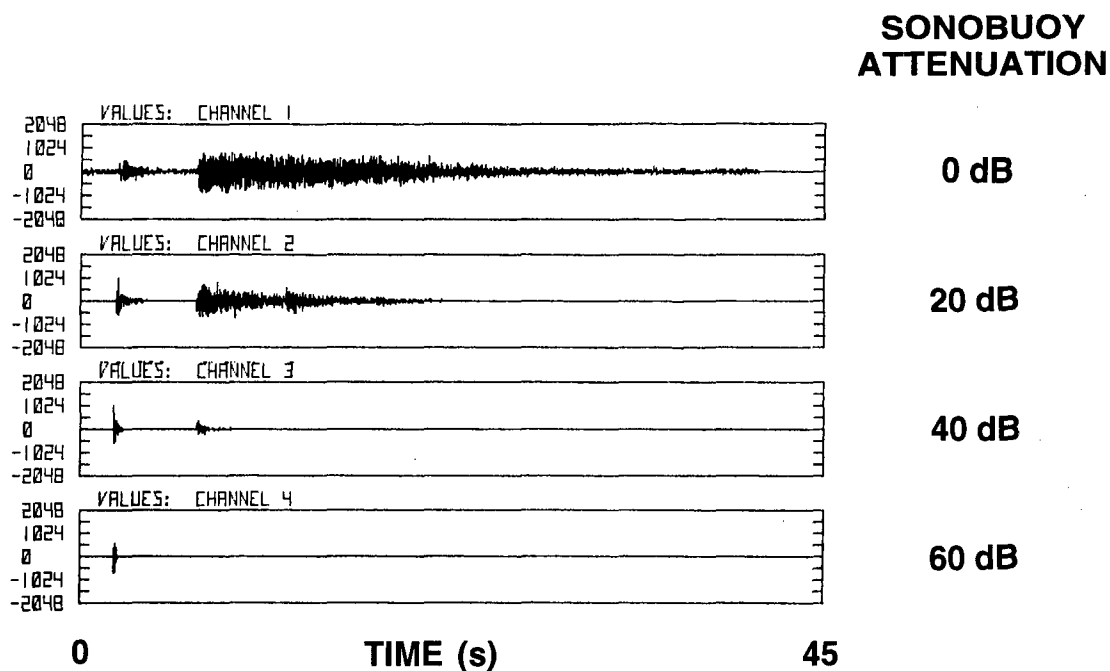
SONOBUOY ATTENUATION

Fig. 2 — Sample near real time plot of digitized reverberation received from differently attenuated sonobuoys (Flight 7, Site C)
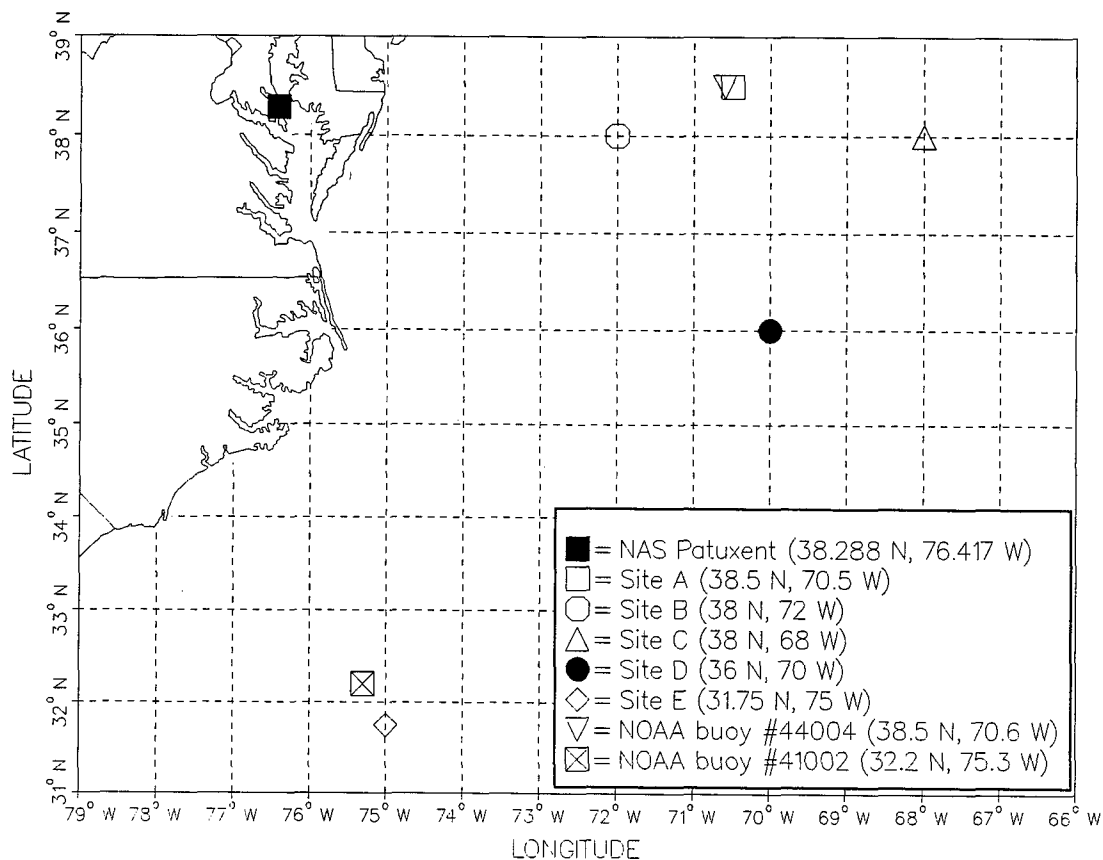

Fig. 3—The locations of the test sites and the NOAA meteorological buoys

Table 1 — Summary of Flights and Test Sites

1988 Julian Day	Date	Comex (Z)	Finex (Z)	Flight No.	Site	Ocean depth (m)	Sea state	Wind speed @ 19.5 m reference height (m/s)
095	4 APR	1645	1925	1	A	3000	2-3	9.5*
099	8 APR	1530	1655	2	A	3000	4	14.5*
099	8 APR	1710	1850	2	B	3000	4	18.0
102	11 APR	1530	1700	3	A	3000	2-3	8.5*
103	12 APR	1520	1630	4	A	3000	3	8.5*
103	12 APR	1700	1910	4	C	4500	3	7.0
105	14 APR	1535	1700	5	A	3000	3	12.5*
105	14 APR	1740	1935	5	D	4500	2	12.5
106	15 APR	1545	1920	6	E	3600	2-3	8.5*
109	18 APR	1515	1915	7	C	4500	4	15.5

* derived from NOAA meteorological buoy data

sites, most likely attributable to the location of the test sites in relation to the Gulf Stream. Appendix A presents all the individual sound speed profiles for each flight and test site.

DATA ANALYSIS

The raw reverberation data sets gathered during the tests were analyzed for surface scattering strengths.

First, the data were bandpass filtered into four octave bands: 50-100 Hz (Band 1), 100-200 Hz (Band 2), 200-400 Hz (Band 3), and 400-800 Hz (Band 4). Next, the data were calibrated to absolute reverberation level by correcting for sonobuoy attenuation, sonobuoy frequency response, and filtering bandwidth.

The source levels used in this analysis were linearly interpolated from the octave band source levels of Gaspin and Shuler (1971), and the units were converted from dB re: 1 erg/cm^2/Hz @ 100 yd to dB re: $(1\mu\text{Pa})^2$/Hz @ 1 m. Within the frequency bands analyzed, Gaspin and Shuler's source levels are in good agreement with the source levels measured by Chapman (1988).

The analysis of the data for surface scattering strengths was performed by using NRL's Direct Path Software Package (DP). DP combines raw data and modeled information to calculate scattering strengths. The raw data provide net reverberation levels (total measured reverberation levels minus ambient noise). The geometric terms of two-way transmission loss and scattering area are modeled by ray-tracing signal propagation from the source to the surface and from the receiver to the surface, then matching the source and receiver rays by horizontal range. With this information, DP then solves the active form of the sonar equation for scattering strength:

$$SS = RL - SL + 2TL - 10 \log (\text{Area}),$$

where

SS = surface backscattering strength in dB,

RL = the reverberation level (in dB re: $(1\mu\text{Pa})^2$/Hz) after background noise has been subtracted,
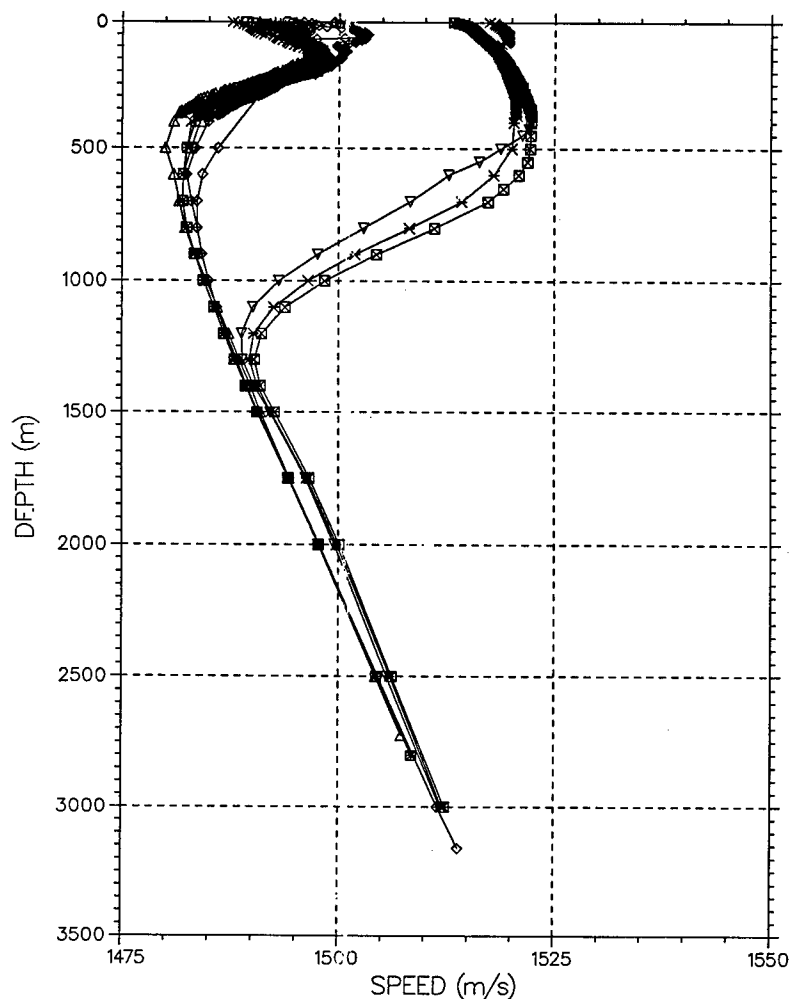
Fig. 4—The sound speed profiles of all
the flights and test sites

SL = the source level in dB re: $(1\mu Pa)^2/Hz$,

TL = propagation loss in dB, and

Area = the estimated scattering area on the sea surface in m^2.

Two points concerning the scope of the analysis need to be mentioned here. First, only the 20 and 40 dB buoys' data have been analyzed for scattering strengths because, for direct path work, the 0 dB buoys were almost always saturated by the received signal, while the 60 dB buoys reached system noise level too quickly. Second, because the method of deploying SUS was inexact, source-receiver separations were larger than desired. Incorporated into the analysis are only those shots for which the test geometry remained reasonably monostatic.

DP was thus used to extract surface scattering strengths from the reverberation data received by the 20 and 40 dB buoys, for each shot of every flight and test site, for all four octave bands. After this, for

each shot of every flight and site that met the above criteria, the scattering strength curves of the 20 and 40 dB sonobuoys were coupled to make a single scattering strength curve for that shot. This was done for all four processing bands. Next, having produced a single scattering strength curve for each shot of every flight and site (for all four processing bands), an average scattering strength curve for each processing band was computed by linearly ensemble averaging all shots for each site (per flight). Finally, the average scattering strength curves were plotted.

Coupling a shot's 20 and 40 dB scattering strength curves was accomplished by aligning, in time, the shot's 20 and 40 dB reverberation time series with each other. It was then determined when the last time was reached at which the 40 dB sonobuoy's received reverberation was valid, meaning that it had not yet reached system noise level, while it had simultaneously matched the reverberation level of the 20 dB sonobuoy at that time. This time was then mapped into a corresponding grazing angle, θ. For grazing angles above this θ, scattering strength values were more accurately calculated from the 40 dB sonobuoy's data; for grazing angles below this θ, scattering strength values were more accurately calculated from the 20 dB sonobuoy's data. If, past the determined time, it was judged that the reverberation curve of the 40 dB sonobuoy lay roughly on top of the 20 dB sonobuoy's reverberation curve, then the 40 dB sonobuoy's scattering strength curve was used as the coupled scattering strength curve.

The wind speed data gathered from the P-3A and the NOAA meteorological buoys were analyzed to provide an environmental descriptor to compare against the measured surface scattering strengths. The P-3A obtained wind speed and air temperature data at its flight altitude and ocean surface temperature from the AXBTs. The meteorological buoys gathered wind speed and air temperature data while simultaneously measuring ocean surface temperature. Both buoy and aircraft wind speed data were corrected to a standard height of 19.5 m using the atmospheric model of Smith (1981, 1988). The corrected wind speeds derived from the meteorological buoys' data were in good agreement with the wind speeds derived from the aircraft's data. Results from the meteorological buoys reflected the general trend present in the aircraft's more frequently sampled data. Figure 5 demonstrates this relationship for a sample flight and site. Time averages were taken over both the P-3A and the meteorological buoys' corrected wind speed data to give the average wind speeds to be used as environmental descriptors. For the aircraft's wind speed data, time averages of each flight and test site were computed. Comparable time averages of the meteorological buoys' wind speed data were computed by linearly averaging together the wind speed data that lay within the time span during which the aircraft wind speed data were taken. It should be noted that, for three sites on four different flights, wind speed data from the meteorological buoys were not available. Where possible, the scattering strength results are presented in comparison with the wind speeds derived from meteorological buoy data. A fuller discussion of the comparison between aircraft and meteorological buoy corrected wind speed data is provided in Appendix B.

RESULTS

For nearly three decades, the U.S. Navy has based its predictions of low-frequency surface backscatter on the empirically derived formula of Chapman and Harris (1962). The Chapman-Harris experiment was performed over a 52-h period during which the wind speeds varied from 0 to 15 m/s; the data were measured in octave frequency bands from 400 to 6400 Hz. Additional tests performed by Chapman and Scott (1964) extended the measurements to 100 Hz. Since then there have been few experiments to confirm the Chapman-Harris results, particularly for high wind speeds and low frequencies. This experiment was one of a series of tests designed to investigate surface backscatter over a range of wind speeds and frequencies.

Recently, NRL has conducted a series of deep-ocean, ship-based surface scattering tests as part of the Critical Sea Test (CST) program. Results from the first four CST exercises have been used by Ogden
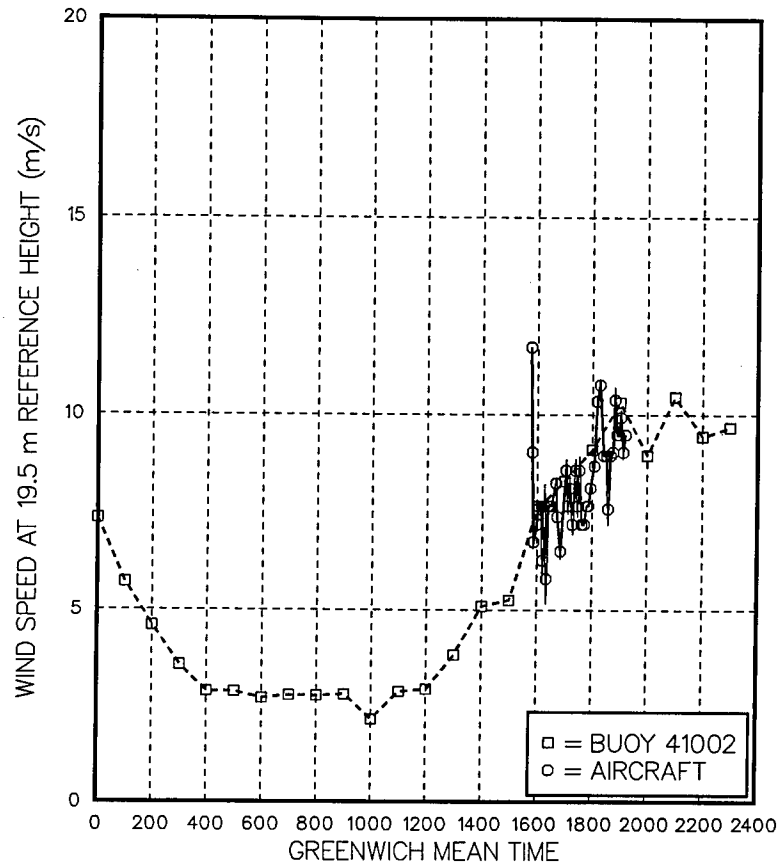
Fig. 5—Comparison between the corrected wind speeds from a NOAA meteorological buoy and the corrected wind speeds from the test aircraft (flight 6, Site E)

and Erskine (1992) to devise a new empirical algorithm for low-frequency surface backscattering strengths based on measurements taken during sea states 1 to 4.5 (wind speeds approximately 3 to 14 m/s at 19.5-m reference height). The CST results of Ogden and Erskine indicate that there are probably at least two major physical mechanisms producing low-frequency sea surface backscatter. For relatively calm seas (sea state 2 or less), for all frequencies below 1 kHz, as well as higher wind speeds at frequencies generally below 200 Hz, the scattering appears consistent with air-water interface backscatter and is adequately described by first order perturbation theory (see, for example, Thorsos 1990). For rougher seas (sea states 3 and above), especially for frequencies above about 300 Hz, the backscatter is reasonably well described by the Chapman-Harris empirical formula. This scattering is caused by a different mechanism, probably subsurface bubble scatter (Henyey, 1991; McDonald, 1991). In between, there appears to be an ill-defined "transition region" in which the scattering strength does not depend in a simple fashion on wind speed and frequency.

The present measurements provide additional data that cover octave bands in the frequency regime of 50 to 800 Hz for wind speeds from 7 to 18 m/s. Although ten surface scattering strength data sets were obtained from this analysis, we only discuss eight of them. The data from Flight 2, Site A and Flight 4, Site A did not contain 40 dB buoy reverberation, so the resulting scattering strength curves are too limited in angular range to warrant close examination. The eight results were obtained for wind speeds of 7.0, 8.5, 9.5, 12.5, 15.5, and 18.0 m/s. We compare these results with several formulations:

- perturbation theory (air-water interface scatter) based on a simple Phillips spectrum (Phillips, 1958), which results in no wind speed or frequency dependence,

- the Chapman-Harris (C-H) empirical formula, and

- the Ogden-Erskine (O-E) empirical algorithm.

The frequencies used as inputs to the C-H and O-E algorithms were the geometric means of the frequency bands used in the data analysis. Also, it should be noted that the measured surface scattering strengths discussed below are considered to have an absolute error of ± 5 dB.

Figure 6 shows measured surface scattering strengths at 7.0 m/s mean wind speed and the corresponding 7.0 m/s empirical predictions of Chapman-Harris and Ogden-Erskine, respectively. We note that, at this low wind speed, for all bands, the O-E scattering strengths are essentially the same as perturbation theory (Fig. 7). The measured scattering strengths are anywhere from 3 to 10 dB higher than the perturbation theory and O-E predictions across all four frequency bands. The measured results are 4 to 8 dB higher than the C-H prediction within Band 1 and 1 to 5 dB higher than C-H within Band 2. Band 3's results are in good agreement with C-H, being no more than 3 dB higher. Band 4's results are generally 1 to 2 dB lower than the C-H prediction. Chapman-Harris is more accurate than Ogden-Erskine for this low wind speed case, except in Band 1. This may be because the mean wind speed lies just below the transition region in the O-E empirical algorithm, even though the estimated sea state (3) at the site would place the O-E prediction in that transition region. This may point to the importance of sea state as an environmental descriptor over that of mean wind speed.

Figure 8 presents measured surface scattering strengths at 8.5 m/s mean wind speed and the corresponding 8.5 m/s empirical predictions of C-H and O-E. The measured scattering strengths increase monotonically with mean grazing angle from 7° to 30° and exhibit a slight, generally monotonic increase in frequency of about 5 to 10 dB from Band 1 to Band 4. Comparison of these results with a first-order perturbation theory prediction (Fig. 7) shows that all the measured results are higher (anywhere from 1 to 10 dB) than the prediction for air-water interface backscatter. The measured results agree with C-H within Band 1, and tend to be about 3 dB lower than C-H within Bands 2-4. The measured results tend to be within 1 to 4 dB higher than O-E in Bands 1 to 2. Band 3 is generally 4 dB higher than O-E, and Band 4 is about 2 dB higher. Still, Odgen-Erskine appear to be more accurate than Chapman-Harris.

Another 8.5 m/s mean wind speed case is given in Fig. 9. Within Bands 1 and 2, the O-E scattering strengths are the same as perturbation theory (Fig. 7). The measured scattering strengths have the same general shape as the empirical predictions. However, there is no general, monotonic increase in scattering strength with frequency, i.e., the results are essentially frequency independent. In Bands 1 and 2, the measured results are 3 to 6 dB higher than O-E. In Band 3, the results are 1 to 4 dB higher than O-E, while Band 4 is 1 to 4 dB lower than O-E. Using C-H, the data are 0 to 4 dB higher in Band 1, 0 to 3 dB lower in Band 2, 2 to 6 dB lower in Band 3, and 5 to 10 dB lower in Band 4. An important point to make in this case concerns the apparent frequency independence of the scattering strength results. Although the mean wind speed of these data is 8.5 m/s, we judged the sea state to be between 2 and 3. Looking at the wind history of these data (see Fig. B6 in Appendix B), one can see that the wind speeds preceding that at the data collection site (by about 4 to 6 h) are significantly lower (around 5 to 6 m/s). If these earlier wind speeds (approximately sea state 1) are the driving force behind this site's scattering strengths, then one would expect perturbation-like (i.e., frequency-independent) scattering. This is what one sees in the data. Thus, the importance of wind history as an environmental factor in scattering strengths may be demonstrated here.
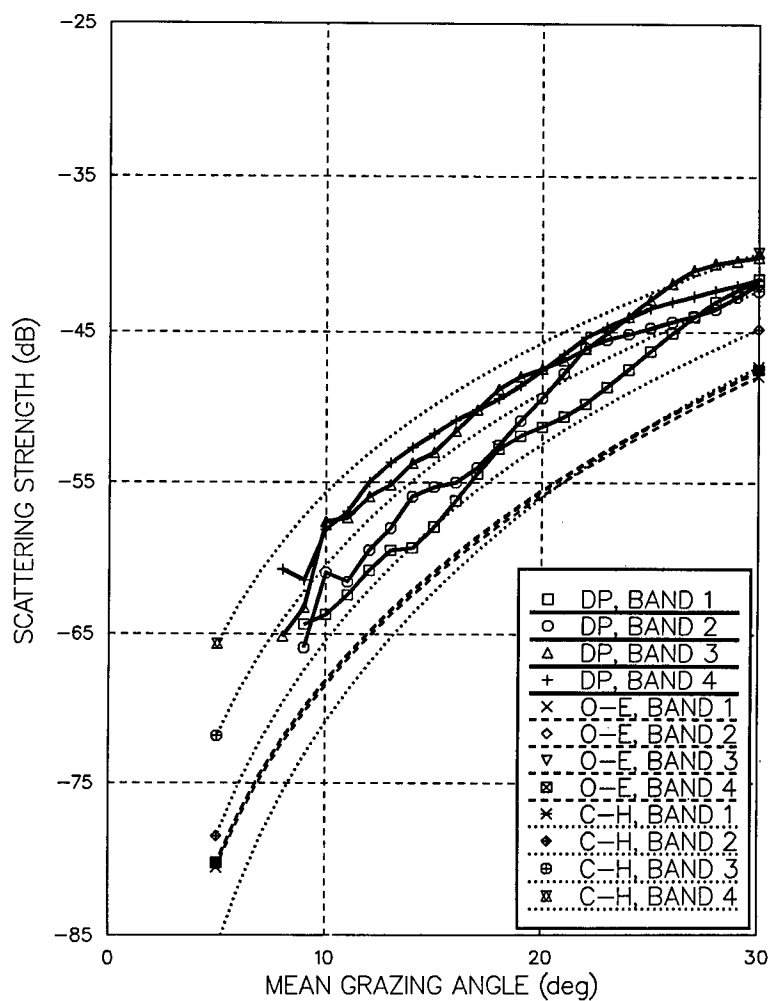
Fig. 6—Flight 4, Site C, 7.0 m/s mean wind speed measured surface scattering
strengths (solid lines) compared to both the Ogden-Erskine empirical algorithm
(dashed lines) and the Chapman-Harris empirical formula (dotted lines)
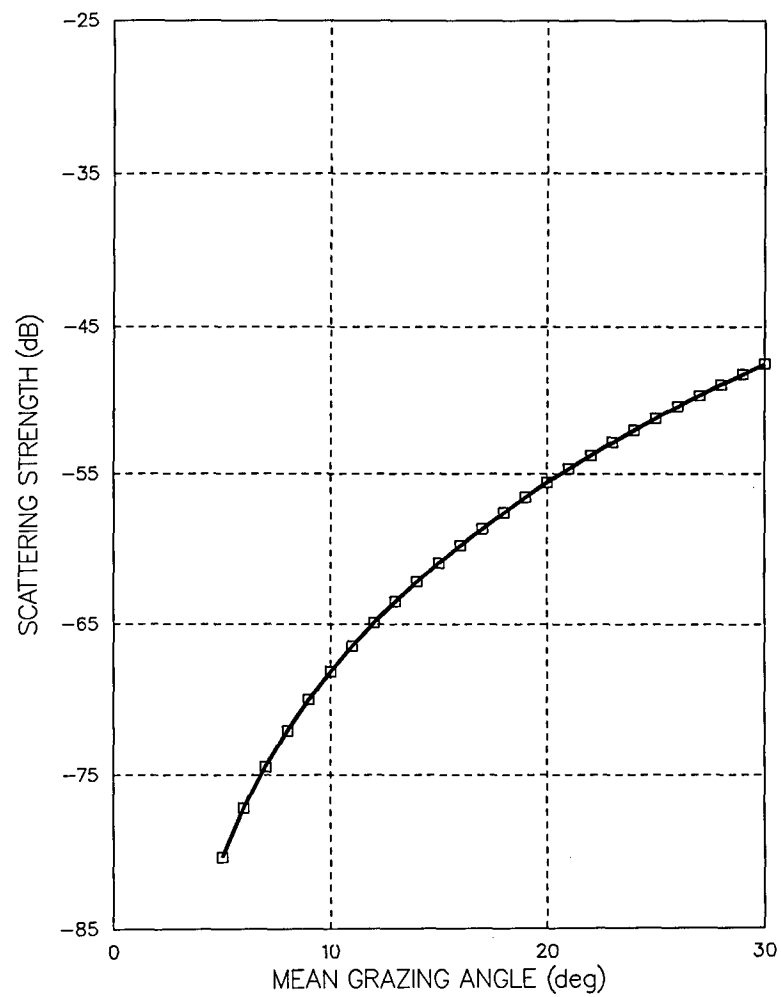
Fig. 7—Surface scattering strength curve predicted
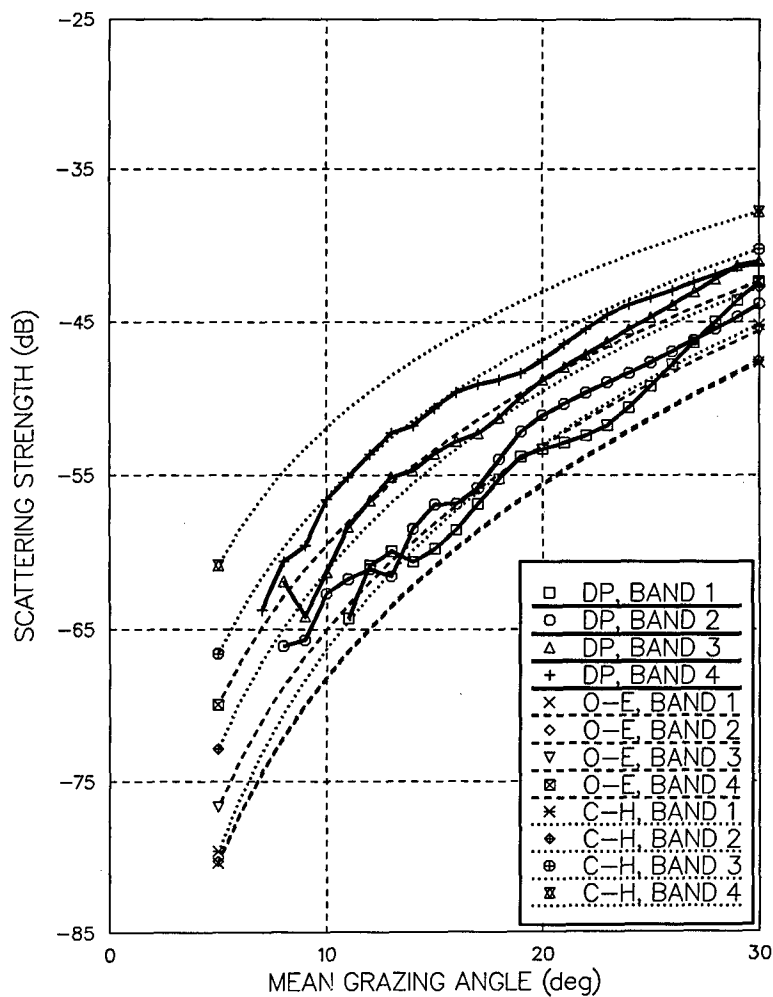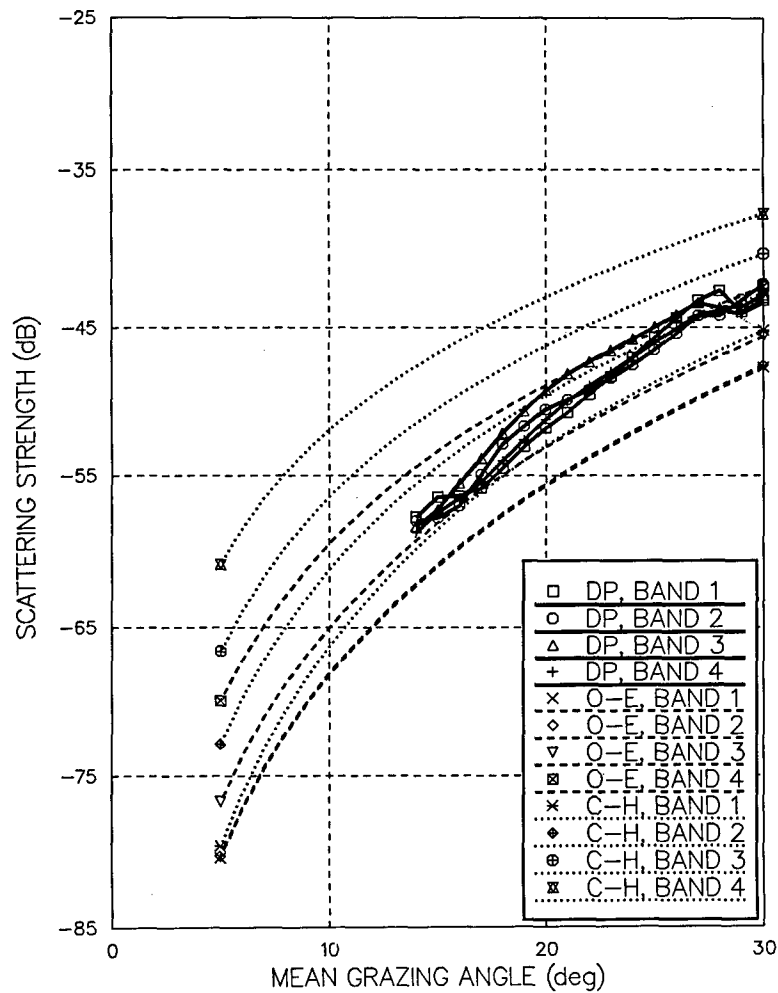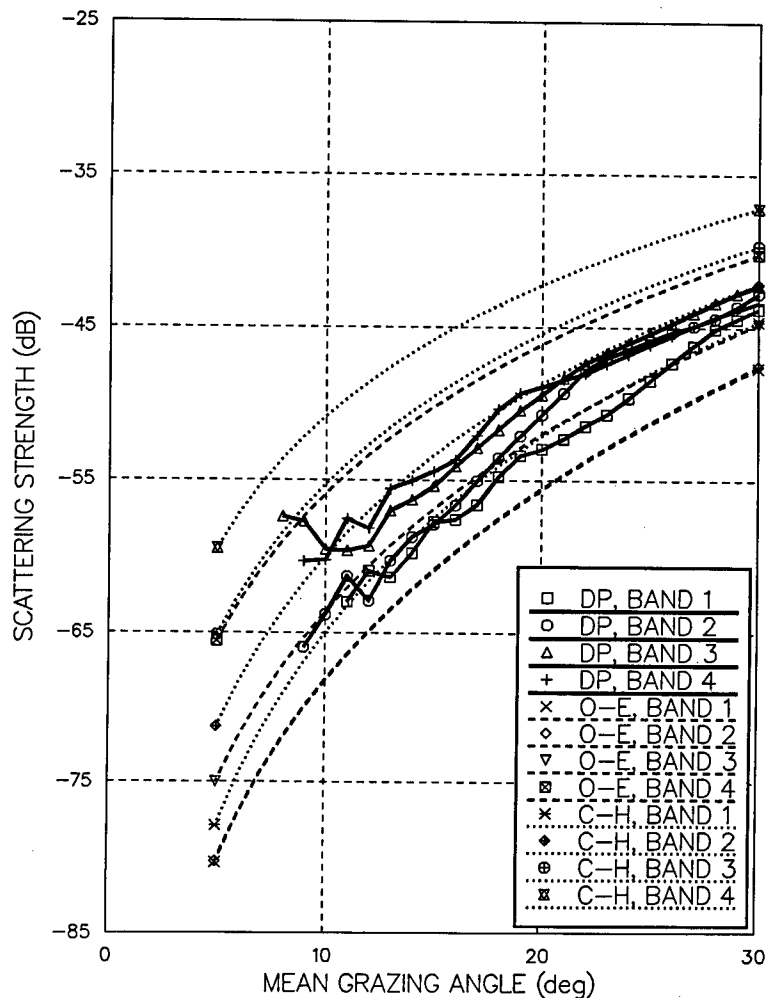by perturbation theory

Fig. 8—Flight 3, Site A, 8.5 m/s mean wind speed measured surface scattering
strengths (solid lines) compared to both the Ogden-Erskine empirical algorithm
(dashed lines) and the Chapman-Harris empirical formula (dotted lines)

Fig. 9—Flight 6, Site E, 8.5 m/s mean wind speed measured surface scattering
strengths (solid lines) compared to both the Ogden-Erskine empirical algorithm
(dashed lines) and the Chapman-Harris empirical formula (dotted lines)

Figure 10 presents surface scattering strengths at 9.5 m/s wind speed and the corresponding 9.5 m/s empirical predictions of C-H and O-E. We note here, too, that within Bands 1 and 2, the O-E scattering strengths are the same as perturbation theory. The results in Band 1 lie within 1 dB of C-H and are about 2 to 4 dB higher than O-E. The results in Band 2 are about 1 to 5 dB lower than C-H and are about 2 to 5 dB higher than O-E. The C-H prediction is generally 3 to 7 dB higher than the results in Band 3, while O-E is generally 1 to 3 dB lower. In Band 4, C-H predicts scattering strengths that are generally 5 to 10 dB higher than the results, whereas O-E predicts scattering strengths that are 3 to 5 dB higher. This case appears to be in the transition region where the scattering strengths are just beginning to show a frequency dependence. This is consistent with the estimated sea state of 2 to 3, which is low for a measured wind speed of 9.5 m/s.
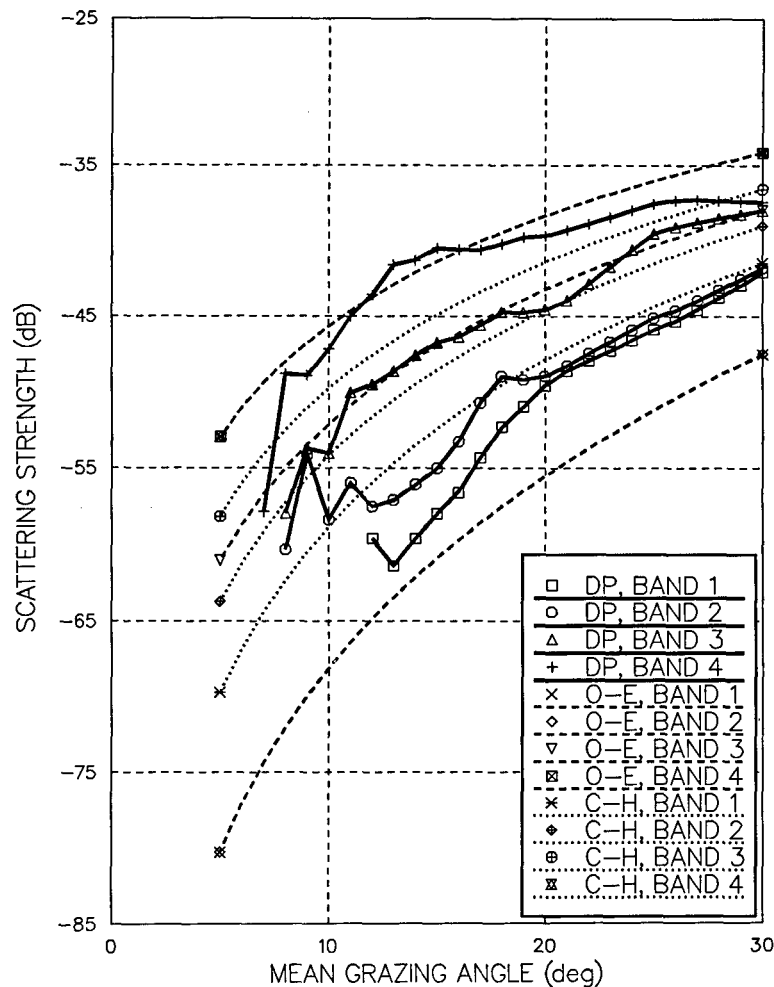

Fig. 10—Flight 1, Site A, 9.5 m/s mean wind speed measured surface scattering strengths (solid lines) compared to both the Ogden-Erskine empirical algorithm (dashed lines) and the Chapman-Harris empirical formula (dotted lines)

Figure 11 shows measured surface scattering strengths at 12.5 m/s mean wind speed and the corresponding 12.5 m/s empirical predictions of C-H and O-E. We note that, within Band 4, the C-H and O-E scattering strengths are the same, while within Bands 1 and 2, the O-E scattering strengths are the same as perturbation theory (Fig. 7). The measured 12.5 m/s scattering strengths show that, at the two highest frequency bands, the measured results are generally in good agreement with O-E (within about 1 dB, except at the highest grazing angle where small residual sonobuoy saturation effects may be present, thus causing a lowering of the measured scattering strengths). At the two lowest frequency bands, where the results fall into the O-E perturbation theory regime (Band 1) or the O-E transition regime (Band 2), the measured results are slightly above O-E predictions by about 3 to 5 dB and below C-H empirical predictions by about 1 to 5 dB. For the lowest frequency band, the measured scattering strengths nearly agree with C-H (within about 2 dB) at the highest grazing angle (near 30°) and nearly agree with perturbation theory levels (within about 2 dB) at the lowest measured grazing angles (around 13°). The measured scattering strengths at intermediate grazing angles do not agree with either C-H or perturbation theory.
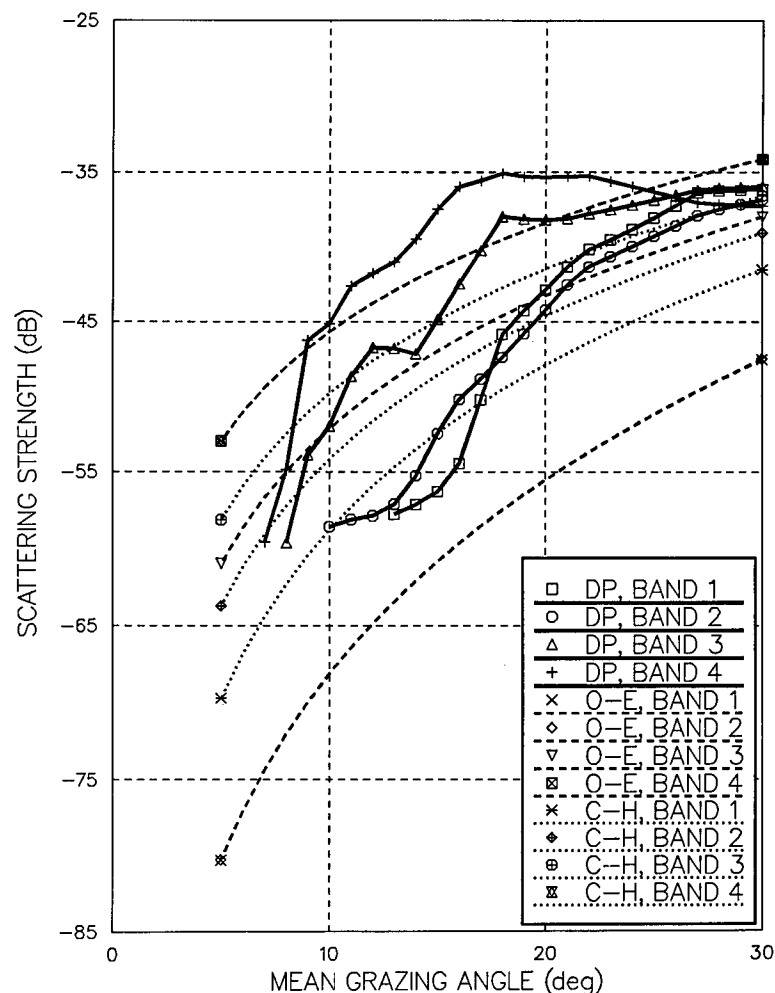

Fig. 11—Flight 5, Site D, 12.5 m/s mean wind speed measured surface scattering strengths (solid lines) compared to both the Ogden-Erskine empirical algorithm (dashed lines) and the Chapman-Harris empirical formula (dotted lines)

Another 12.5 m/s mean wind speed case is given in Fig. 12. The results for the two lowest frequency bands do not agree with O-E or perturbation theory. At higher grazing angles (20° to 30°), the scattering strengths for Band 1 are approximately 6 dB higher than C-H and in Band 2 are generally 3 dB higher. As in Fig. 11, the lower grazing angle results suggest a trend toward perturbation-type scattering, even though in this case the match at these angles is not good. The results in Band 3 are matched well in the intermediate grazing angles ranging from 11° to 16° by C-H (within about 1 dB), but are around 1 to 3 dB higher than C-H at 20° and above. The flattening at higher grazing angles (possibly caused by sonobuoy saturation effects) is present here as well. The O-E prediction for Band 3 is about 2 to 5 dB lower than the results at grazing angles of 20° and above. The scattering strengths in Band 4 do not agree with either C-H or O-E, which are the same in this case. Band 4 also exhibits a flattening in scattering strength levels at grazing angles higher than 20°.
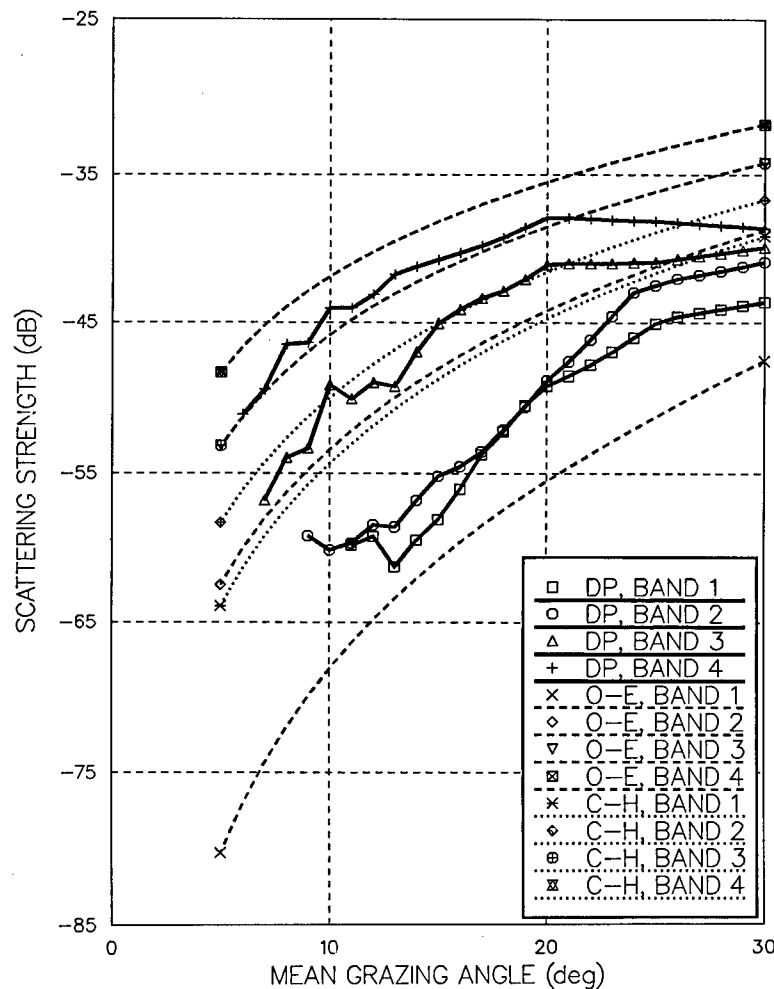

Fig. 12—Flight 5, Site A, 12.5 m/s mean wind speed measured surface scattering strengths (solid lines) compared to both the Ogden-Erskine empirical algorithm (dashed lines) and the Chapman-Harris empirical formula (dotted lines)

Figure 13 presents measured surface scattering strengths at 15.5 m/s mean wind speed and the corresponding 15.5 m/s empirical predictions of C-H and O-E. We find that the measured data are about 2 to 5 dB lower than O-E and C-H at the two highest frequency bands, but have generally the same slopes as O-E and C-H (except that at about 20° and higher grazing angles the data may be slightly low because of residual sonobuoy saturation effects; alternatively, this depression may be a real effect at higher frequencies and higher grazing angles). The results for the two lowest frequency bands exhibit an apparent grazing angle-dependent effect that for higher grazing angles (near 30°) the measured scattering strengths approach C-H levels, but remain about 4 to 5 dB lower than C-H, while at lower grazing angles (10° to 15°) the results approach the perturbation theory prediction (Fig. 7), but remain slightly above it by 1 to 5 dB.
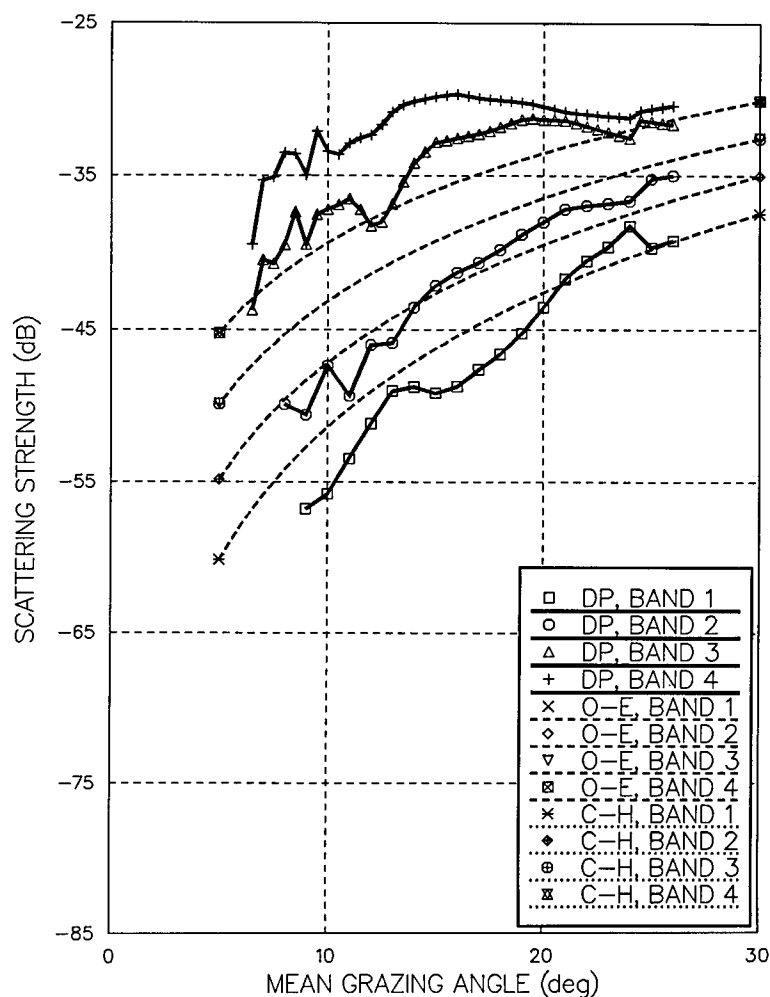

Fig. 13—Flight 7, Site C, 15.5 m/s mean wind speed measured surface scattering strengths (solid lines) compared to both the Ogden-Erskine empirical algorithm (dashed lines) and the Chapman-Harris empirical formula (dotted lines)

Figure 14 shows measured surface scattering strengths at 18.0 m/s mean wind speed and the corresponding 18.0 m/s empirical predictions of C-H and O-E. At this high wind speed, the C-H and O-E empirical predictions are identical for all four measurement frequency bands. The measured scattering strengths within Bands 3 and 4 are generally about 5 dB higher than the empirical predictions (C-H, O-E) for low grazing angle (7° to 15°), but exhibit a flattening of slope with increasing grazing angle at higher grazing angles (15° to 30°). The measured scattering strengths within Bands 1 and 2 are within 1 to 3 dB of the empirical predictions (C-H, O-E) at the highest grazing angles (15° to 30°) and fall off slightly (by 1 to 5 dB) relative to C-H, O-E at the lowest measured grazing angles (around 8°), with the lowest frequency data falling off fastest.

Fig. 14—Flight 2, Site B, 18.0 m/s mean wind speed measured surface scattering strengths (solid lines) compared to both the Ogden-Erskine empirical algorithm (dashed lines) and the Chapman-Harris empirical formula (dotted lines)

SUMMARY OF SCATTERING STRENGTH MEASUREMENT RESULTS

We have measured sea surface scattering strengths at acoustic frequencies below 1 KHz by using an airborne scattering technique over the western Atlantic Ocean in 1988. Scattering strengths have been measured in four octave bands (50-100 Hz, 100-200 Hz, 200-400 Hz, and 400-800 Hz) over a variety of sea conditions from wind speeds of 7.0 to 18.0 m/s (referenced to 19.5 m height). Measured scattering strength results have been compared to predictions of air-water interface scattering (perturbation theory) and the empirical formulations of C-H and O-E. Figure 15 shows our airborne scattering data sets in relation to the wind speed vs frequency scattering domain of O-E. Our measurements extend into the high wind speed regime above 15 m/s and into the low-frequency regime below 200 Hz, where existing data sets are sparse. Additional high wind and low frequency data sets are needed to better characterize surface scattering. The present measurements have yielded the following insights into surface scattering:

- At wind speeds above 15 m/s and grazing angles below 15°, scattering strengths for frequencies above about 200 Hz may be somewhat higher than predicted by either the C-H or the O-E empirical algorithms.

- At wind speeds above about 10 m/s, frequencies above about 200 Hz, and grazing angles above 15°, scattering strengths may exhibit a flattening of slope with increasing grazing angle, relative to the empirical predictions (C-H, O-E). Possibly, this flattening may be an instrumental effect.

- At moderate wind speeds below 10 m/s (e.g., 8.5 m/s), the present measurements are in better agreement (at all measured frequency bands from 50-800 Hz) with the empirical predictions of O-E than with those of C-H. From Fig. 15, we see that the present 8.5 m/s surface scatter measurements reside either in the perturbation theory regime (below 200 Hz) or in the O-E "transition region" for which the C-H empirical formula generally predicts the scattering strengths to be too high.

- It is known from other work on surface scattering (see, for example: Ogden-Erskine, 1992) that the wind speed alone is a poor predictor of surface scattering strengths and that wind history in some form needs to be incorporated into the prediction algorithms. Generally, these data support that conclusion. Further analysis of this data set may help to clarify the role of wind history in surface scatter predictions.

AIRBORNE TECHNIQUE: LESSONS LEARNED

The April 1988 surface backscattering tests provided a means of testing an airborne technique for measuring reverberation. A number of lessons concerning this technique were learned from these tests.

- Simultaneous launching of the sonobuoys is needed. As noted before, launching sonobuoys one at a time resulted in at least 100-m separations between each. Consequently, the geometry between each sonobuoy and a particular "shot" is not identical, which affects scattering strength analysis when aligning reverberation by time. Launching all the sonobuoys at one time would minimize this problem.

- The aircraft's OTPI proved to be insufficient for accurate shot deployment during the tests. As a result, it became necessary to use the smoke markers as guides to the proper time to launch each SUS. Although preferable to relying solely on the OTPI, the differential drift between the smoke markers and the sonobuoys left doubt as to the accuracy of this method. Because the OTPI proved
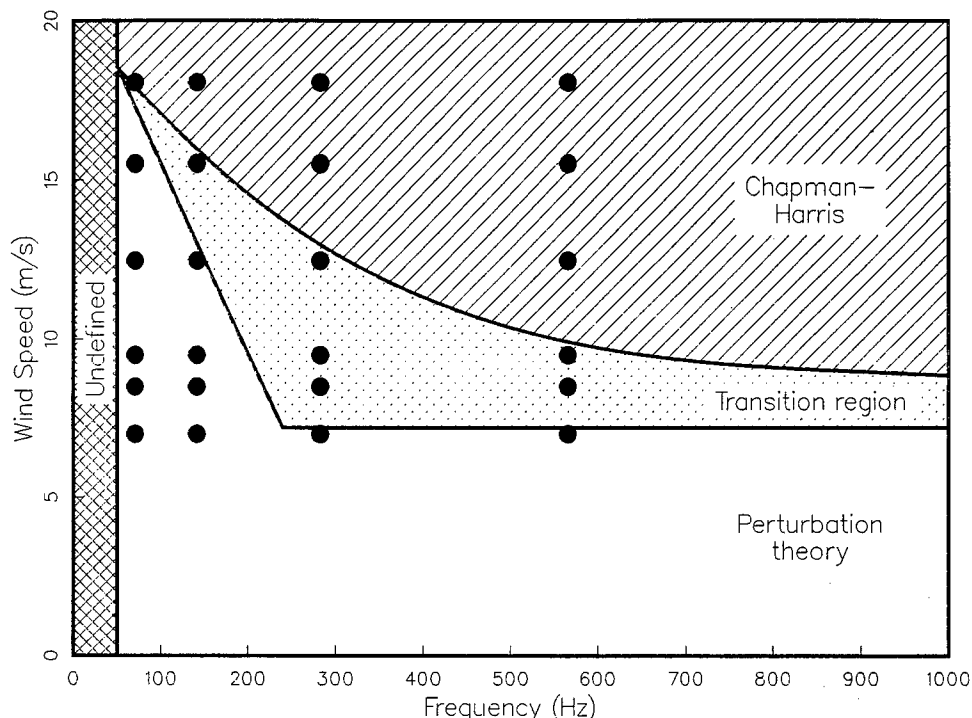
Fig. 15—1988 airborne surface scatter measurement data sets compared to the
Ogden-Erskine empirical algorithm wind speed vs frequency domain (solid dots
indicate present measurement sets)

to be unreliable, flying the modified figure-eight pattern perpendicular to the line made by the
smoke markers and sonobuoys was not very successful. If it is necessary to deploy the sonobuoys
along a line rather than in a single location, superior results are likely to be achieved by flying a
pattern parallel to the sonobuoy line rather than perpendicular.

• Absolute calibration problems were encountered when replaying the analog tapes. Replaying was
sometimes necessary because the A/D converter only had four channels. For those times when
more than four sonobuoys had been launched, the extra channels could not be digitized in real
time. It is preferable to digitize all the channels during a test rather than deal with the problems
of A/D conversion after a test.

• As mentioned above, 0 dB sonobuoys are not useful in direct path analysis because they are almost
always saturated by the received signal. It is not necessary to use 0 dB sonobuoys for this type
of experiment. (This conclusion would be different for tests carried out in shallow water, if the
objective was to measure more distant reverberation rather than local scattering.)

• This set of tests has pointed out the need to carefully calibrate the attenuated sonobuoys so that
their respective received reverberation signals match up in level.

• The wind speeds measured from aircraft appear to be reliable if appropriate corrections are made
for aircraft altitude and the performance of the aircraft sensors as a function of aircraft speed and
local conditions.

ACKNOWLEDGMENTS

REFERENCES

Chapman, N.R. 1988. "Source Levels of Shallow Explosive Charges," *J. Acoust. Soc. Am.* **84**(2), 697-702.

Chapman, R.P. and H. D. Scott. 1964. "Surface Backscattering Strengths Measured over an Extended Range of Frequencies and Grazing Angles," *J. Acoust. Soc. Am.* **36**, 1735-1737.

Chapman, R.P. and J. H. Harris. 1962. "Surface Backscattering Strengths Measured with Explosive Sound Sources," *J. Acoust. Soc. Am.* **34**(10), 1592-1597.

Gaspin, J.B. and V.K. Shuler. 1971. "Source Levels of Shallow Underwater Explosions," Naval Ordnance Laboratory Report NOLTR 71-160.

Henyey, F.S. 1991. "Acoustic Scattering from Ocean Microbubble Plumes in the 100 Hz to 2 kHz Region," *J. Acoust. Soc. Am.* **90**(1), 399-405.

McDonald, B.E. "Echoes from Vertically Striated Subresonant Bubble Clouds: A Model for Ocean Surface Reverberation," *J. Acoust. Soc. Am.* **89**(2), 617-622.

Naval Oceanographic Office. 1987. "Data Base Description for Generalized Digital Environmental Model (GDEM) Historical Ocean Profile (HOP) Subset."

Ogden, P.M. and F. T. Erskine. 1992. "An Empirical Prediction Algorithm for Low-Frequency Acoustic Scattering Strengths," NRL Report NRL/FR/5160--92-9377.

Phillips, O.M. 1958. "The Equilibrium Range in the Spectrum of Wind-Generated Waves," *J. Fluid Mech.* **4**, 426-434.

Smith, S.D. 1981. "Coefficients for Sea-Surface Wind Stress and Heat Exchange," Bedford Institute of Oceanography Report BI-R-81-19.

Smith, S.D. 1988. "Coefficients for Sea Surface Wind Stress, Heat Flux, and Wind Profiles as a Function of Wind Speed and Temperature," *J. Geophys. Res.* **93**, 15467-15472.

Thorsos, E.I. 1990. "Acoustic Scattering from a 'Pierson-Moskowitz' Sea Surface," *J. Acoust. Soc. Am.* **88**, 335-349.

Urick, R.J., *Principles of Underwater Sound*, 3rd Ed. (McGraw-Hill Book Company, New York, New York, 1983).

Appendix A

MEASURED SOUND SPEED PROFILES

Figures A1 through A10 show the sound speed profiles used during the analysis of each flight and site. Ocean depth is measured in meters; sound speed is measured in meters per second (m/s).

From the figures, the regimes of the in-situ and archival data can clearly be seen. That portion of the figures extending down to about 300 to 400 m is the heavily-sampled, in-situ data from the AXBTs. Below that is the much less sampled archival data from the GDEM database.

Also apparent from the figures are the two distinct types of sound speed profiles encountered in the region of the test sites. The sound speed profiles for Flights 5 and 6 (Figs. A7-A9) indicate a warmer ocean temperature than that of the other flights. In comparison with other flights, their sound speeds are 10 to 35 m/s greater in the upper 1000 m of ocean. Interesting to note as well are both the sound speed profiles from Site C (Flight 4, Fig. A6 and Flight 7, Fig. A10). Both flights exhibit sound speeds that are about 5 m/s greater in the top 100 to 150 m of water than are those of Flights 1 to 3 and Flight 4, Site A (see Fig. 4 of the main report). We postulate that these increases in sound speed are explained by the proximity of the test sites to the Gulf Stream.
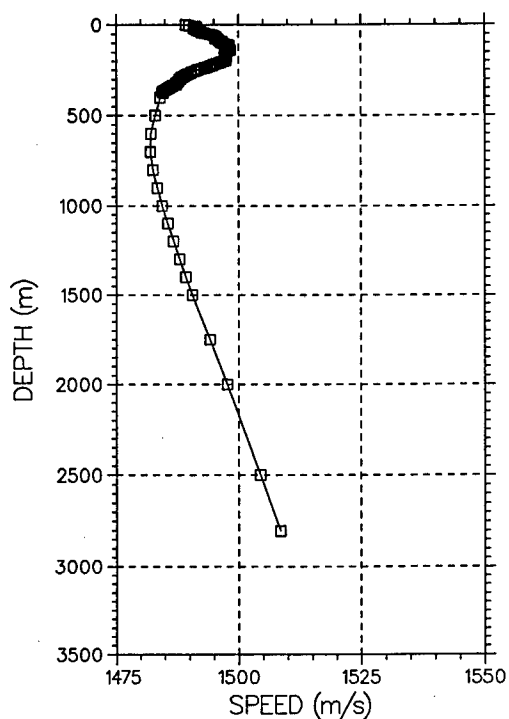
Fig. A1—Flight 1, Site A's composite sound
speed profile (in-situ extended via the GDEM
database)
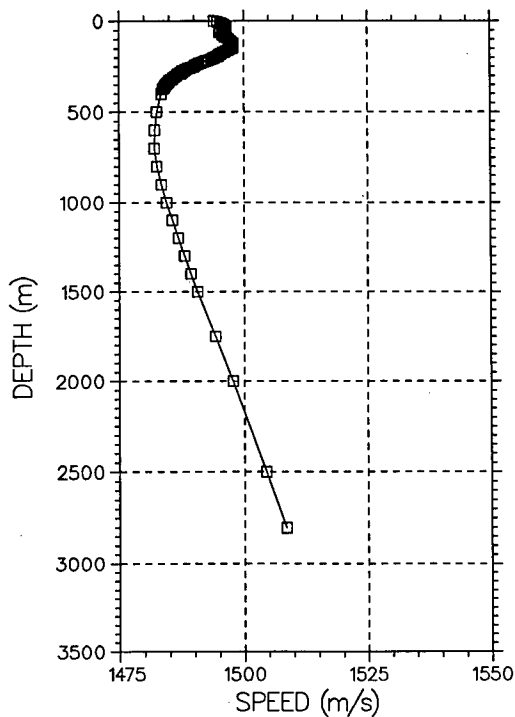
Fig. A2—Flight 2, Site A's composite sound
speed profile (in-situ extended via the GDEM
database)
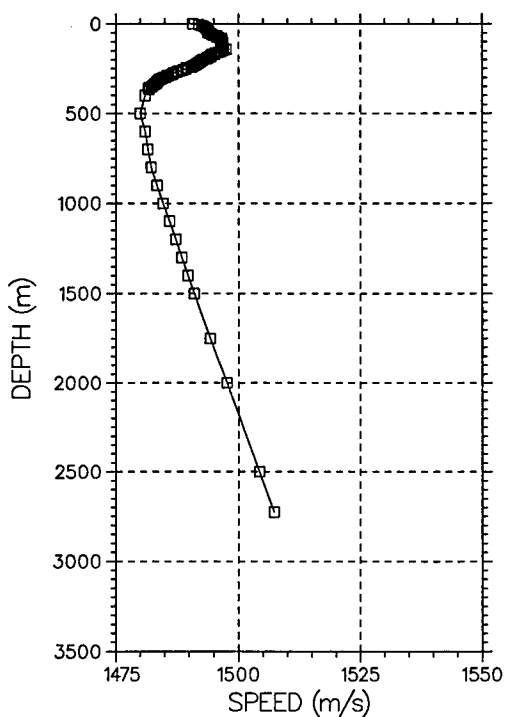
Fig. A3—Flight 2, Site B's composite sound
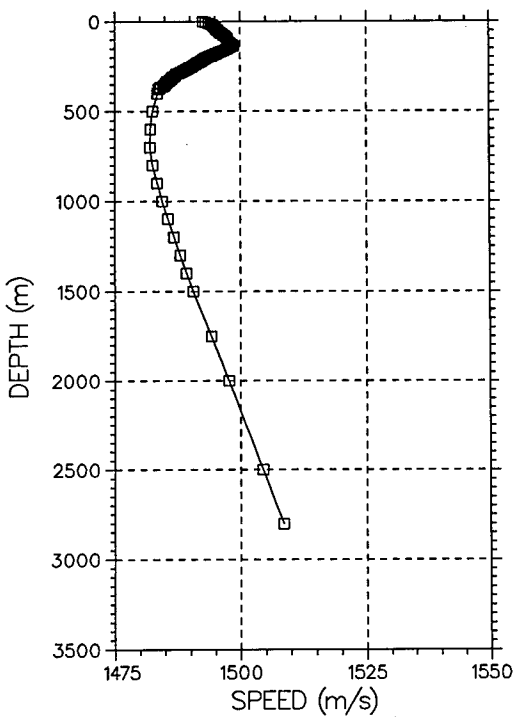speed profile (in-situ extended via the GDEM
database)

Fig. A4—Flight 3, Site A's composite sound
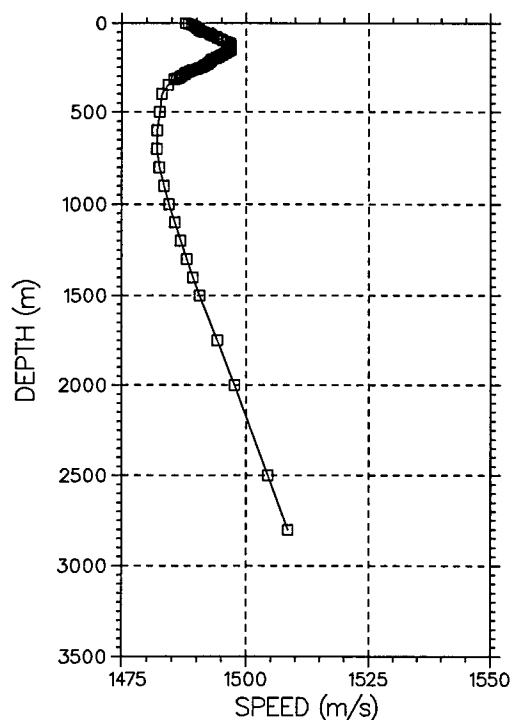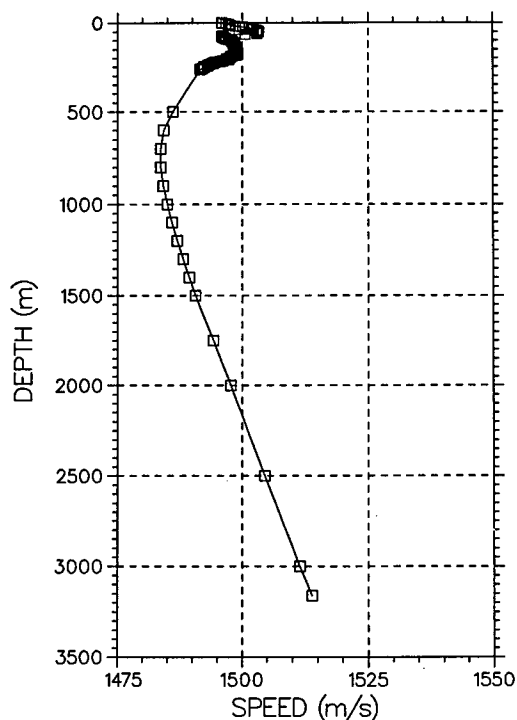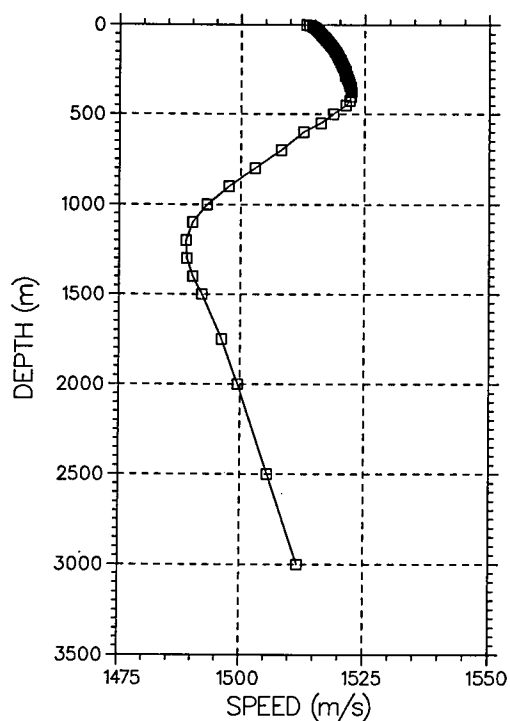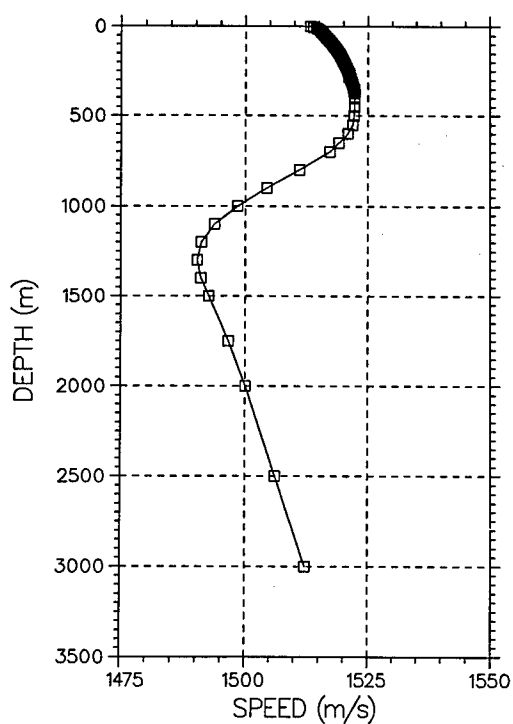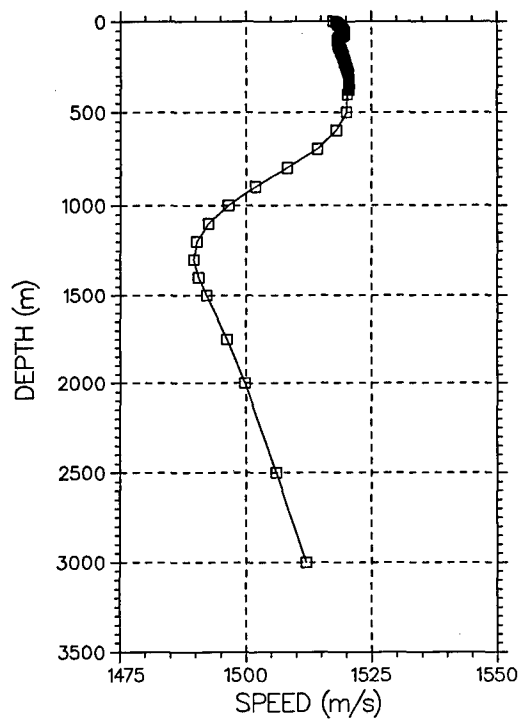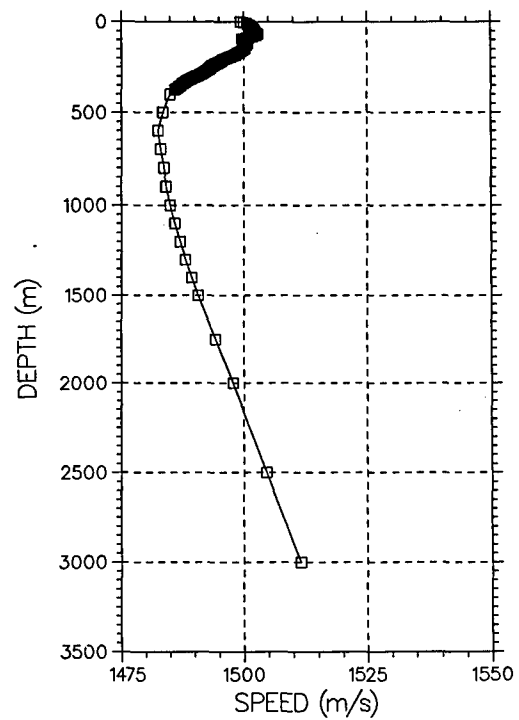speed profile (in-situ extended via the GDEM
database)

Fig. A5—Flight 4, Site A's composite sound speed profile (in-situ extended via the GDEM database)

Fig. A6—Flight 4, Site C's composite sound speed profile (in-situ extended via the GDEM database)

Fig. A7—Flight 5, Site A's composite sound speed profile (in-situ extended via the GDEM database)

Fig. A8—Flight 5, Site D's composite sound speed profile (in-situ extended via the GDEM database)

Fig. A9—Flight 6, Site E's composite sound speed profile (in-situ extended via the GDEM database)

Fig. A10—Flight 7, Site C's composite sound speed profile (in-situ extended via the GDEM database)

Appendix B

MEASURED WIND SPEED RESULTS

Figures B1 through B6 show (plotted together) the corrected wind speed data from the aircraft and the NOAA meteorological buoys. This is done for the flights and sites where comparison between the two is possible because the distances between the sites and the buoys were small. Primarily this meant Site A, which was about 9 km from buoy No. 44004, but we also include Site E, which was about 57 km from buoy No. 41002. The solid lines represent aircraft wind speeds; the dashed lines represent buoy data.

Flight 1, Site A's aircraft wind speed data are least like buoy 44004's wind speed data. The aircraft's wind speeds are, on the average, about 2 m/s higher than the buoy's wind speeds.

For Flights 2 through 5, Site A's aircraft wind speed data are all in very good agreement with buoy 44004's wind speed data. On average, the aircraft's wind speeds are 0.5 m/s higher than the buoy's wind speeds for Flight 2, less than 0.5 m/s lower than the buoy's wind speeds for Flight 3, and less than 1.0 m/s higher than the buoy's wind speeds for Flights 4 and 5.

The comparison between Flight 6, Site E's aircraft data and buoy 41002's data is the best. On average, the aircraft's wind speed data are approximately 0.5 m/s less than the buoy's wind speed data. Most visibly apparent in this case is the pairing between the general trend (of increasing wind speed) in the aircraft's wind speed data and the meteorological buoy's data.

A possible extension to these comparisons is the use of corrected meteorological buoy wind speed data to provide wind speed histories of test sites that lie in sufficient proximity to the meteorological buoys. Our corrections show the closeness between corrected aircraft wind speeds and corrected buoy wind speeds. Our conclusion is that these wind speeds are reasonably reliable values. Thus, it seems reasonable that the corrected buoy wind speeds for times preceding those of the actual tests are also reasonably reliable. With these "extra" wind speeds available from the buoys, it becomes possible to construct wind speed histories for test sites, and Ogden and Erskine (1992) suggest that wind history is a more useful environmental descriptor in predicting surface scattering strengths than is instantaneous wind speed alone.
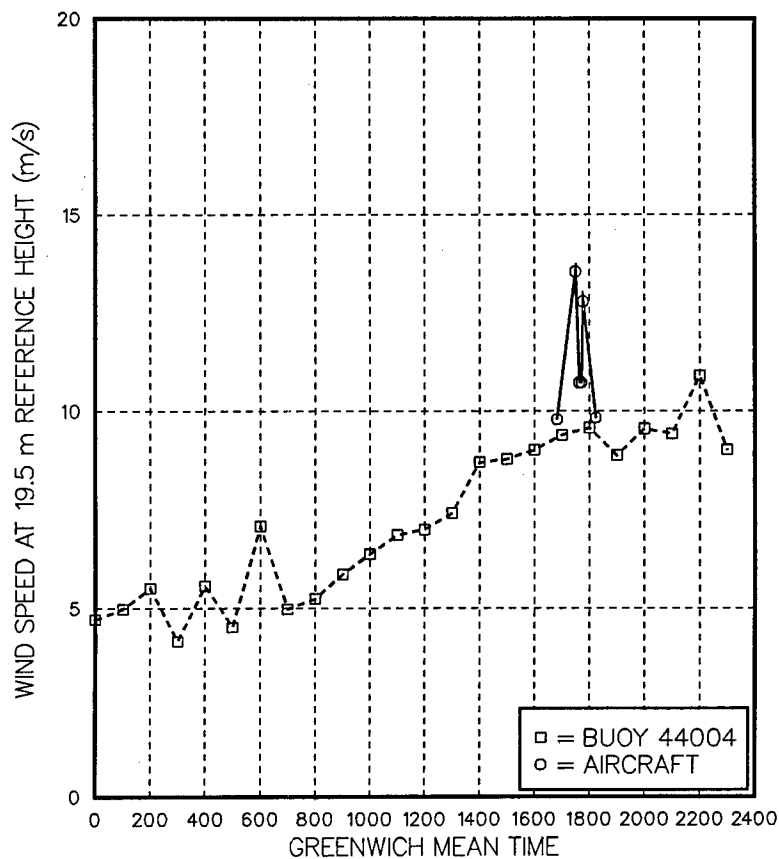
Fig. B1—Comparison between the corrected wind speeds from meteorological buoy #44004 and the corrected wind speeds from the test aircraft, for Flight 1, Site A

Fig. B2—Comparison between the corrected wind speeds from NOAA meteorological buoy #44004 and the corrected wind speeds from the test aircraft, for Flight 2, Site A
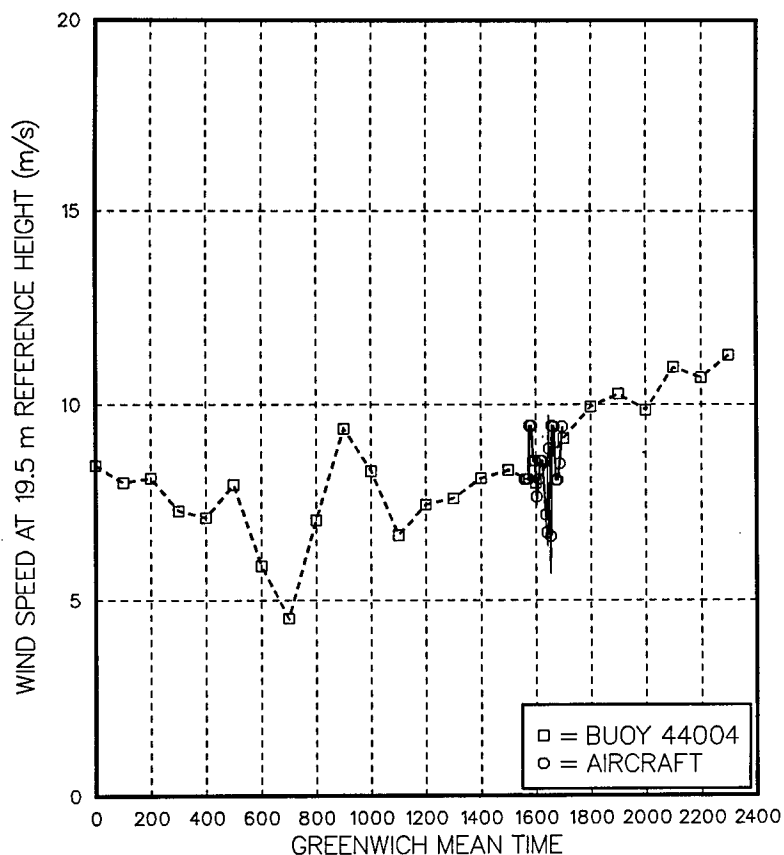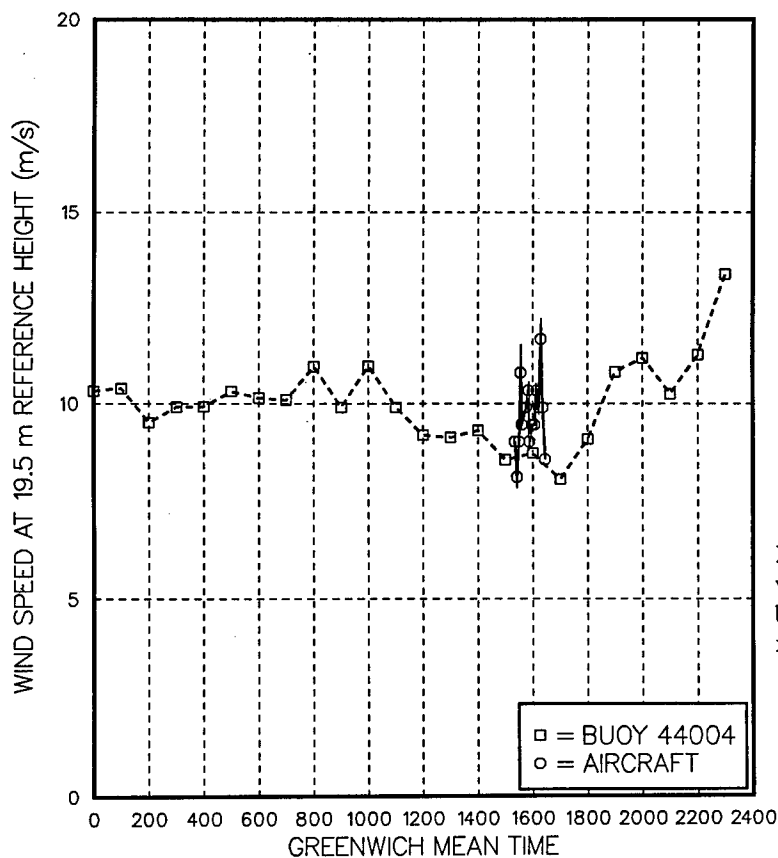
Fig. B3—Comparison between the corrected
wind speeds from NOAA meteorological
buoy #44004 and the corrected wind speeds
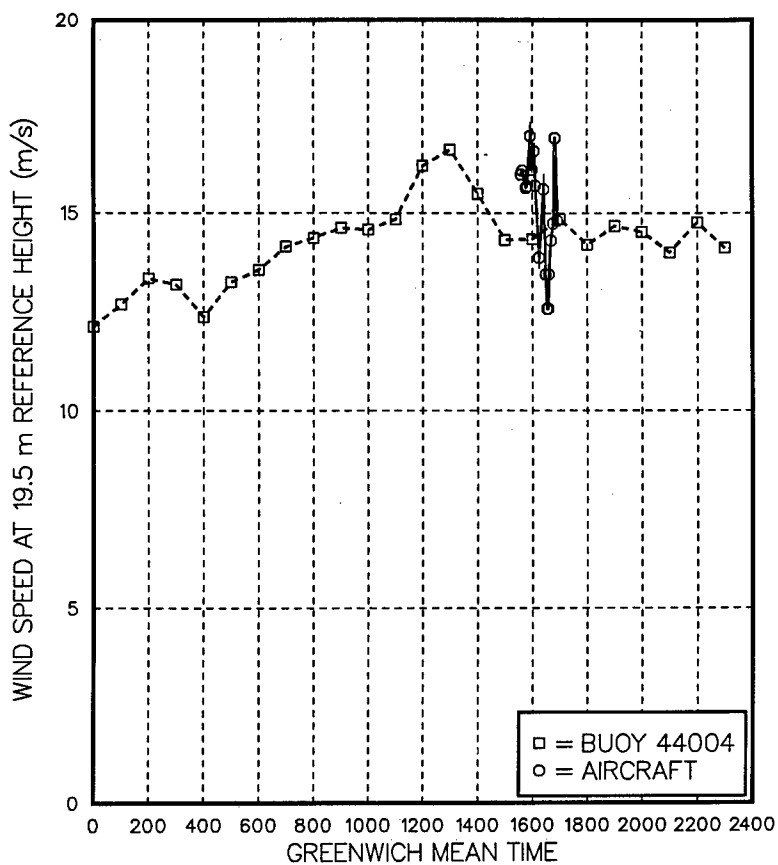from the test aircraft, for Flight 3, Site A

Fig. B4—Comparison between the corrected
wind speeds from NOAA meteorological
buoy #44004 and the corrected wind speeds
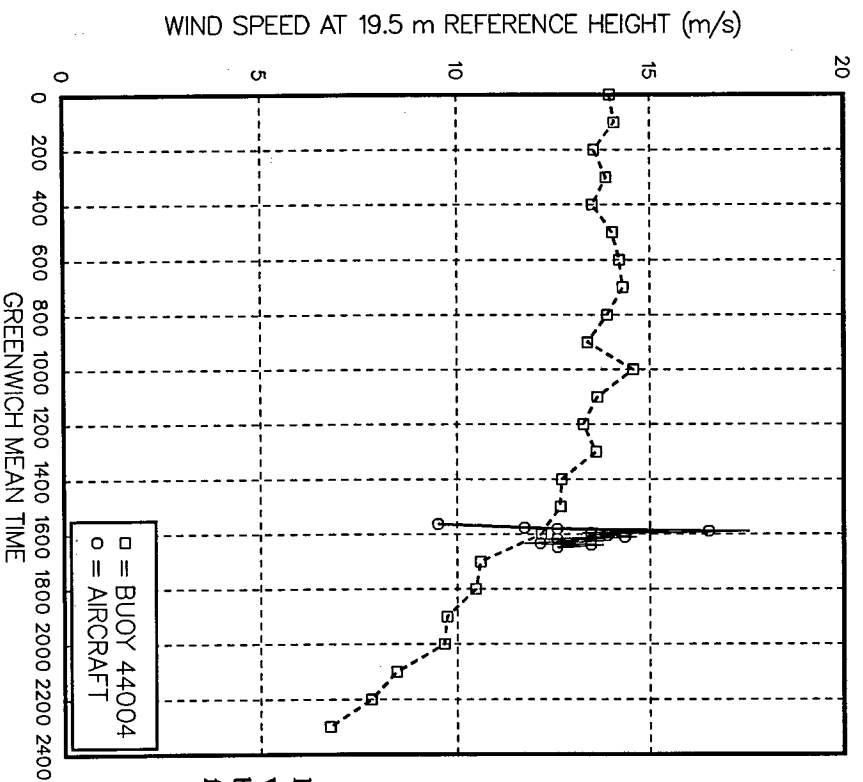from the test aircraft, for Flight 4, Site A

Fig. B5—Comparison between the corrected wind speeds from NOAA meteorological buoy #44004 and the corrected wind speeds from the test aircraft, for Flight 5, Site A
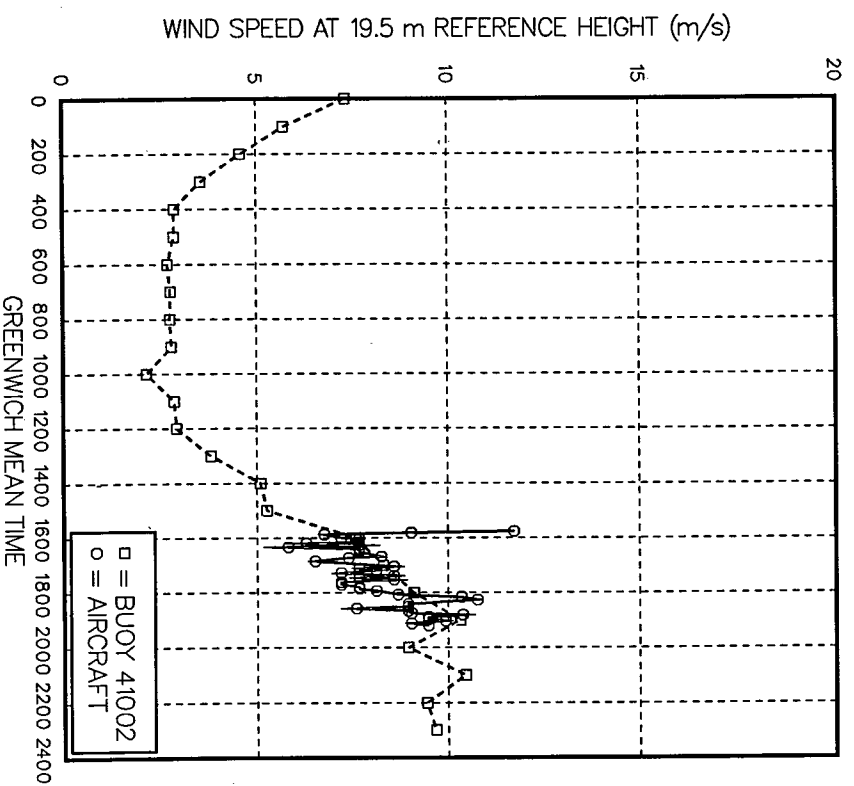

Fig. B6—Comparison between the corrected wind speeds from NOAA meteorological buoy #41002 and the corrected wind speeds from the test aircraft, for Flight 6, Site E